16th World Conference on Earthquake, 16WCEE 2017

Santiago Chile, January 9th to 13th 2017

Paper N° 119

Registration Code: S-S1463234767

ASSESSMENT OF COLLAPSE POTENTIAL OF SPSW HAVING INFILL PLATES DESIGNED USING TWO DIFFERENT PHILOSOPHIES

R. Purba(1), M. Bruneau(2)

(1) Assistant Professor, Department of Civil Engineering, Universitas Bandar Lampung, Indonesia. Email: ronnypurba@ubl.ac.id
(2) Professor, Department of Civil, Structural and Environmental Engineering, University at Buffalo, U.S.A. Email: bruneau@buffalo.edu

Abstract

Research was conducted to assess collapse potential of steel plate shear walls (SPSWs) having infill plates designed to resist different percentages of the applied lateral loads. This paper first describes the development of component strength deterioration models that are needed to be able to perform the collapse assessment of SPSWs. Collapse assessment was then conducted on SPSWs designed neglecting the contribution of their boundary moment resisting frames to resist story shear forces as well as on SPSWs designed considering the sharing of story shear forces between the boundary frames and infill plates. Based on these assessments, seismic performance factors (i.e., response modification coefficient (*R*-factor), system overstrength Ω_0 factor, and deflection amplification C_d factor) for both types of SPSWs were identified and compared. Adjustments to improve collapse performance and factors that affect collapse potential were presented. Collapse fragility curves for archetypes with various structural configurations were investigated. Findings from these analyses demonstrate that the infill plates of SPSWs should be designed to resist the total specified story shears, and that SPSWs designed by sharing those story shears between the boundary frame and infill plates will undergo significantly larger and possibly unacceptable drifts.

Keywords: steel plate shear walls; deterioration modes; collapse potential; seismic performance factors; FEMA P695.

1. Introduction

In current building codes for the design of steel plate shear walls [1, 2], ambiguity exists as to whether contribution of the boundary frame moment resisting action to the global plastic lateral strength of steel plate shear walls (SPSW) can be taken into account when it comes to resisting lateral loads or whether the infill plates of SPSW must be designed to resist the entire lateral loads. In the latter case, the seismic behavior of SPSW has traditionally benefited from the overstrength introduced in the horizontal and vertical boundary elements (HBE and VBEs), but questions have arisen in recent years suggesting that explicitly allowing sharing of lateral loads between the boundary frame and infill plates as a means to optimize SPSW designs might be cost-effective, but of unknown consequences on behavior [3, 4]. Based on their experiences designing multistory SPSWs, the latter researchers assigned a certain percentage of the total design base shear to be resisted by the boundary frame and the remaining portion resisted by the infill plates. The former researchers, on the other hand, developed a procedure to design SPSW considering boundary frame moment resisting action that would theoretically achieve a balanced (optimum) design minimizing overstrength of the system. Both design approaches however use the same response modification coefficient (i.e., *R*-factor) as that of conventional SPSWs, implicitly assuming that both types of SPSWs would have comparable seismic performance. Qu and Bruneau [3] however commented on the possible need to design the optimized systems to a different *R*-factor, based on limited results showing that SPSWs designed to have lateral loads shared by infill plates and boundary frame experienced larger drifts compared to conventional SPSWs.

This paper investigates the seismic performance of SPSWs having infill plates designed per these two different philosophies. Using the FEMA P695 methodology [5], which defines the performance in terms of collapse potential under maximum considered earthquake (MCE) ground motions, the assessment is first conducted on SPSWs designed neglecting the contribution of their boundary moment resisting frames to resist story shear forces. In other words, infill plates are designed to resist the entire story shear forces. Then, this assessment of collapse potential is repeated for SPSWs designed considering the sharing of story shear forces between the boundary frames and infill plates. Based on these assessments, seismic performance factors (i.e., response modification coefficient (R-factor), system overstrength Ω_0 factor, and deflection amplification C_d factor) for both types of SPSWs are identified and compared.

2. Development of Nonlinear Models for Collapse Simulation

Deterioration material models for SPSW components (i.e., strips and boundary elements) were developed based on testing data of a total of 36 conventional unstiffened slender-web SPSW specimens. The specimens varied from single- to four-story SPSWs with aspect ratio ranging from 0.7 to 2.2. Both welded and bolted connections were used in these walls, either connecting infill plates by means of fish plates to boundary frames or connecting horizontal to vertical boundary elements. Among the 36 SPSW specimens examined, a large variability of experimental outcomes was observed. To avoid a biased statistical interpretation of cyclic deformation capacity at the ultimate (capping) and failure points, only the specimens that were pushed beyond the ultimate point and exhibited stable deterioration with gradual strength drop were considered, as shown in Table 1 for 17 selected specimens.

Table 1 – List of Steel Plate Shear Walls Tested Specimens [6-9, 15-21]

Researcher	Spec. ID	No. of Stories	Geometric Properties			Type of Connection[1]		Condition at Ultimate			Condition at End			μ[3]
			L_p (mm)	H_s (mm)	Aspect Ratio	Frame	Infill	Mode[2]	V_{max} (kN)	Drift (%)	Mode[2]	V_{end} (kN)	Drift (%)	
Driver *et al*. (1997)	– [a]	4	3050	1776	1.7	W	W	WT	3080	2.2[b]	FBE	2618	4.0[b]	9.0
Lubell *et al*. (2000)	SPSW2	1	900	900	1.0	W	W	FBE	250	4.00	FBE	175	5.0	7.5
Astaneh-Asl and Zhao (2002)	UCB-1	2	– [a]	3100	– [a]	W	W	FBE	4005	3.3[b]	FBE	2403	4.0[b]	5.7
	UCB-2	3	– [a]	2067	– [a]	W	W	FBE	5451	2.2[b]	FBE	4066	3.0[b]	4.3
Behbahanifard et al. (2003)	– [a]	3	3050	1678	1.8	W	W	FBE	3500	2.6[b]	WT	2850	3.7[b]	7.9
Berman and Bruneau (2005)	F2	1	3658	1829	2.0	P	W	WT	620	3.0	WT	420	3.7	12
Vian and Bruneau (2005)	P	1	4000	2000	2.0	W+RBS	W	FBE	1790	2.0	FBE	1650	3.0	10
	CR	1	4000	2000	2.0	W+RBS	W	FBE	2050	2.5	FBE	1340	4.0	13.3
Park *et al*. (2007)	SC2T	3	1750	1100	1.6	W	W	FBE	1663	2.6[c]	FBE	1338	3.8[e]	7.0
Qu *et al*. (2008)	– [a]	2	4000	4000	1.0	W+RBS	W	FBE	4245	3.3[b,d]	WT	2387	5.2[b,d]	10.4
Choi and Park (2008)	FSPW1	3	1650	1075	1.5	W	W	FBE	1392	3.6[c]	FBE	1364	5.2[e]	8.1
	FSPW2	3	2350	1075	2.2	W	W	FBE	1817	4.5[c]	WT	1776	5.6[e]	11.8
	FSPW3	3	2350	1075	2.2	W	W	FBE	1565	2.7[c]	FBE	1100	5.4[e]	10.6
Choi and Park (2009)	BSPW1	3	2350	1075	2.2	W	P	WT	1882	3.6[c]	WT	1200	5.3[c]	11.8
	BSPW2	3	2350	1075	2.2	W	P	WT	1961	3.3[c]	FBE	1055	5.3[c]	11.0
Li *et al*. (2010)	N	2	2140	3250	0.7	W+RBS	W	FBE	1300	4.0[e]	FBE	1105	5.0[e]	12.5
	S	2	2140	3250	0.7	W+RBS	W	FBE	1070	3.0[e]	WT	910	5.3[e]	12.5

Note:
a) Not available b) First story drift c) Top story drift d) Information from phase II (i.e., cyclic test) e) Maximum inter-story drift
1) P = Pin (simple) or partial welded connection; W = Welded (rigid) connection; RBS = Reduced Beam Section
2) WT = deteriorated Web Tearing; FBE = Failure of Boundary Elements
3) $\mu = \Delta_{end}/\Delta_{yield}$

Inferred from the experimental data, among several possible causes, deterioration of structural components that lead to failures of SPSWs consist of deteriorations associated with web tearing (WT) and flexural failure of boundary elements (FBE). The proposed deterioration models were calibrated on 4 selected specimens that represent single- to four-story SPSWs [6, 7, 8, 9]. Each specimen has a unique characteristic for which observation of different scenarios of strength degradation can be made. The single-story specimen [6] exhibited fractures of boundary elements but no fractures of its infill plates that contributed to the specimen strength degradation (i.e., the infill plates exhibited significant plastic deformations instead). The reverse scenario was observed in the three-story specimen [8], where strength deterioration was attributed to web tearing in absence of significant damages to boundary elements. A case for which both fracture of boundary elements and deterioration due to web tearing was reported in [7] for a two-story specimen. While both deterioration modes were also observed in the four-story specimen [9], strength degradation rate and magnitude of this degradation were not as severe as that in the two-story specimen. Considering that the four calibrated specimens already covered the ranges of aspect ratio, number of stories, drift capacities at the ultimate and end conditions, and amount of strength degradation for the specimens reported in Table 1, additional calibration was not conducted and the four calibrated specimens deemed adequate to represent the intended calibration results. Detailed calibration information can be found in [10]. The resulting deterioration models are shown in Fig. 1 for strips and boundary elements.

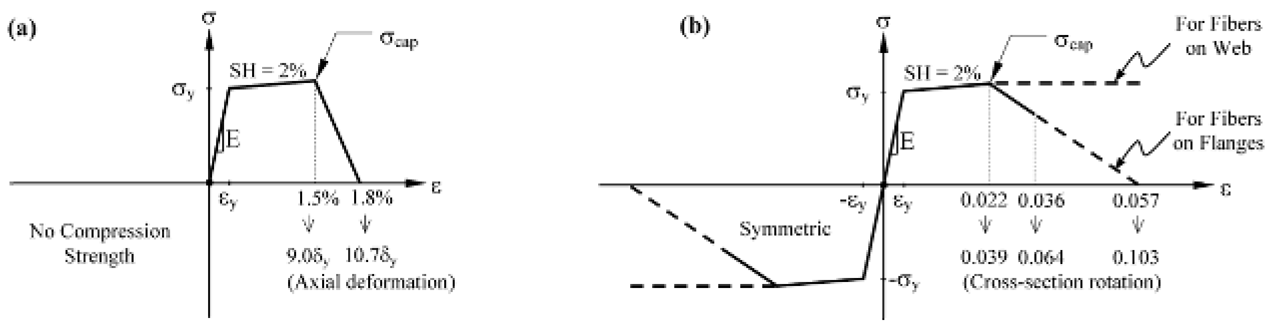

Fig. 1 – Degradation Models: (a) Strips; (b) Boundary Elements

Fig. 2 shows an example two-dimensional nonlinear model for collapse simulation of 3 story SPSW archetypes developed in OpenSees [11]. This dual strip model incorporates an axial hinge at every strip and concentrated fiber plastic hinges (each with 65 fibers across the cross section) at the ends of VBEs and HBEs. Panel zones are not included in this model as their impacts on the global behavior of the model are insignificant. The "gravity-leaning-column" elements are added adjacent to the strip model.

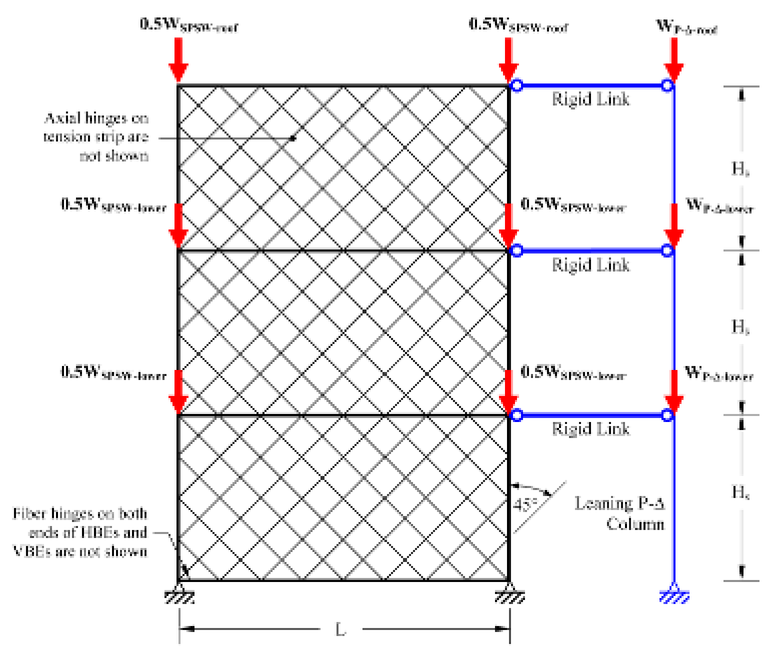

Fig. 2 – Nonlinear Model for Collapse Simulation: Example Structural Model of 3-Story Archetype

3. Development of Steel Plate Shear Walls Archetypes

SPSW archetypes were designed either for the case where the infill plates can resist alone 100% of the specified seismic load without considering boundary frame moment resistance (a.k.a. conventional design with $\kappa = 1.0$) or for the case where SPSW optimized to effectively eliminate overstrength (as a consequence of the boundary frame strength) such that the sum of the strength of boundary frame and infill plates was exactly equal to the required strength to resist the designed lateral loads. This optimum design was defined as the "balanced" design case (i.e., $\kappa = \kappa_{balanced}$) in [3].

For the purpose of quantifying seismic performance factors for SPSWs having infill plates designed to sustain different levels of lateral loads, twelve SPSW archetypes consisting of 3 to 10 stories office buildings were prepared (i.e., 6 archetypes each for conventional and balanced design cases). For convenience, their loading information, floor plans, and elevations were taken as similar to the SAC model building described in the FEMA 355-C document [12]. All SPSWs had moment resisting HBE-to-VBE connections. Both design approaches used the capacity design principle outlined in the AISC 2010 Seismic Provisions to design HBEs and VBEs; and archetypes were explicitly designed to avoid development of in-span hinges per the design procedure addressed in [13]. Two levels of seismic tributary weight were considered, namely low and high seismic weight. Archetypes were sized based on the Design Basis Earthquake (DBE) response spectra specified in the FEMA P695 document for high seismicity (i.e., SDC D_{max}). Story seismic weight and design base shear for each archetypes is shown in Table 2. The resulting sizes of VBEs, HBEs, and infill plate are summarized in Table 3 for the 3-story archetypes, while those for the 5- and 10-story archetypes can be found in [10].

Table 2 – Story Weight and Design Base Shear of SPSW Archetypes

Archetype ID[1]	**Level**	**W_{SPSW} (kips)**	**$W_{P\text{-}\Delta}$ (kips)**	**W_{total} (kips)**	**V_d (kips)**
SW310, SW310K	Roof	63.42	317.41	380.83	154.84
	Lower	58.61	292.99	351.60	
SW320, SW320K	Roof	126.94	253.89	380.83	175.87
	Lower	117.20	234.40	351.60	
SW320KR6	Roof	126.94	253.89	380.83	205.18
	Lower	117.20	234.40	351.60	
SW320KR5	Roof	126.94	253.89	380.83	246.22
	Lower	117.20	234.40	351.60	
SW320G, SW320GK	Roof	126.94	1014.55	1141.49	464.51
	Lower	117.20	937.83	1055.03	
SW520, SW520K	Roof	126.94	253.89	380.83	255.32
	Lower	117.20	234.40	351.60	
SW520G, SW520GK	Roof	126.94	1014.55	1141.49	765.95
	Lower	117.20	937.83	1055.03	
SW1020, SW1020K	Roof	136.00	256.30	392.30	680.88
	Lower	126.25	237.93	364.18	

Note:
W_{SPSW} = Gravity Loads on SPSW
$W_{P\text{-}\Delta}$ = Gravity Loads on P-Δ Leaning Column
W_{total} = Total Seismic Weight for Base Shear Calculation (= $W_{SPSW} + W_{P\text{-}\Delta}$)
V_{total} = Design Base Shear
[1)] ID Convention follows the following example
SW320GKR6 = **S**teel **W**alls | **3** story Archetype | Aspect Ratio **2.0** | High Tributary Seismic Mass (High **G**ravity Loads on Leaning Column) | Design with $\kappa_{balanced}$ | Design with **R** factor of **6** instead of 7

Table 3 – Design Summary of 3-Story SPSW Archetypes for Collapse Assessment

SPSW Components	100% Design Case (κ = 1.0)			Balanced Design Case (κ = $\kappa_{balanced}$)[1]		
	SW310	**SW320**	**SW320G**	**SW310K**	**SW320K**	**SW320GK**
HBE-3	**W14×53** (1.0[a])	**W18×76** (0.99)	**W27×146** (0.96)	**W12×40** (0.95)	**W18×40** (0.99)	**W21×93** (0.96)
HBE-2	**W12×45** (0.99)	**W14×61** (0.99)	**W14×159** (0.96)	**W10×33** (0.95)	**W12×35** (0.98)	**W18×71** (0.97)
HBE-1	**W16×31** (0.98)	**W12×45** (0.95)	**W18×97** (0.97)	**W12×22** (0.94)	**W10×26** (0.95)	**W14×48** (1.0)
HBE-0	**W18×86** (0.94)	**W24×117** (0.98)	**W24×306** (0.97)	**W18×55** (0.96)	**W21×68** (0.98)	**W21×166** (0.98)
VBE-3	**W18×50** (0.96)	**W16×89** (0.98)	**W27×161** (0.98)	**W16×36** (0.98)	**W14×53** (0.94)	**W14×132** (0.99)
VBE-2	**W18×71** (0.98)	**W18×76** (0.99)	**W27×178** (0.95)	**W16×45** (0.96)	**W18×40** (0.98)	**W21×93** (0.96)
VBE-1	**W21×122** (1.0)	**W24×146** (0.96)	**W36×300** (1.0)	**W18×86** (0.96)	**W24×76** (0.96)	**W21×201** (0.97)
t_{w3} (in)	**0.071**	**0.036**	**0.101**	**0.044**	**0.018**	**0.047**
t_{w2} (in)	**0.115**	**0.059**	**0.163**	**0.071**	**0.029**	**0.078**
t_{w1} (in)	**0.141**	**0.072**	**0.203**	**0.087**	**0.035**	**0.094**

Note: a) Value in parenthesis is demand-to-capacity ratio
1) Balanced condition: $\kappa_{balanced}$ = 0.63, L/h = 1.0, $\alpha_{average}$ = 41° (SW310K)
$\kappa_{balanced}$ = 0.49, L/h = 2.0, $\alpha_{average}$ = 44° (SW320K, SW320GK)

4. Collapse Performance Evaluation of SPSW Archetypes

Collapse performance evaluation was conducted according to the guidelines described in the FEMA P695 methodology [5]. The evaluations started by determining uncertainty factors (β_{TOT}) related to SPSW archetypes and nonlinear model. Nonlinear pushover analysis and incremental dynamic analyses (IDA) were performed afterward to obtain system overstrength (Ω_o), period-based ductility (μ_T) factor, median collapse capacity ($\hat{S}_{CT}$), and collapse margin ratios (*CMR*). Spectral shape factor (SSF) values were used to modify the CMR to the adjusted collapse margin ratio (ACMR) which is a function of the archetype fundamental period (T) and μ_T factor. The ground motion records used in the evaluation consisted of 22 "Far-Field" ground motion record pairs (44 individual components) of large magnitude (M > 6.5) from sites located at distances greater than or equal to 10 km from fault rupture [14].

Results of performance evaluations of all archetypes considered are summarized in Table 4. Detail information can be found in [10]. All conventional archetypes passed the performance criterion. The computed ACMR for each archetype was larger than the acceptable $ACMR_{10\%}$ of 2.16. These results indicate that each archetype has a reasonable safety margin against collapse (i.e., a lower probability of collapse) as a result of the overstrength reserve provided by the boundary frame. For this type of SPSW, results indicate that the R factor of 7 used in design is adequate (i.e., satisfied the ACMR requirement). The Ω_o factor for the archetypes considered (based on the pushover analysis results) varied from 2.3 to 3.1. Considering the limited numbers of SPSW archetypes designed in this research, the Ω_o factor of 2.0 can be considered adequate for conventional SPSW. Assuming the inherent damping available in SPSW to be 5% of critical damping, a C_d factor of 7 can be considered for conventional SPSWs. Note that the resulting seismic performance factors for conventional SPSW obtained in this case are somewhat similar to those specified in the ASCE 7-10 (i.e., R, Ω_o, and C_d factors are 7, 2, and 6, respectively).

For the balanced archetypes, except for the 10-story archetype and 5-story archetype design with high seismic weight (i.e., SW1020K and SW520GK), all other archetypes did not meet the performance criterion because their computed ACMR was smaller than $ACMR_{10\%}$. These results indicate that the R factor of 7 used in the initial step to design the balanced SPSW would not lead to an adequate design (i.e., the resulting did not satisfy the ACMR requirement). Design iterations would be required to determine acceptable seismic performance factors for SPSW designed with $\kappa_{balanced}$.

Table 4 - Summary of Performance Evaluation for SPSW Archetypes with Various Structural Configurations

Archetype ID	Pushover Results						IDA Results		Performance Evaluation		
	V_d (kips)	V_{max} (kips)	$\delta_{y,eff}$ (in)	δ_u (in)	$\Omega_0 = V_d/V_{max}$	$\mu_T = \delta_u/\delta_{y,eff}$	$\hat{S}_{CT}$ (g)	CMR = $\hat{S}_{CT}/S_{MT}$	SSF[1]	ACMR[2]	Pass/ Fail[3]
SW310	155	401	2.1	11.7	2.6	5.5	3.14	2.10	1.26	2.64	**Pass**
SW320	176	495	1.8	8.9	2.8	4.9	3.60	2.40	1.25	3.00	**Pass**
SW320G	465	1440	1.8	9.9	3.1	5.5	4.08	2.72	1.26	3.43	**Pass**
SW520	255	578	3.9	16.3	2.3	4.2	3.40	2.42	1.25	3.03	**Pass**
SW520G	766	1924	4.1	19.5	2.5	4.8	4.26	3.03	1.27	3.85	**Pass**
SW1020	681	1975	7.8	40.6	2.9	5.2	3.40	4.08	1.36	5.58	**Pass**
SW310K	155	236	2.1	10.5	1.5	5.0	2.28	1.52	1.25	1.90	**Fail**
SW320K	176	226	1.8	8.6	1.3	4.8	2.29	1.53	1.24	1.90	**Fail**
SW320GK	465	618	1.7	8.9	1.3	5.1	2.32	1.55	1.25	1.93	**Fail**
SW520K	255	254	3.8	16.1	1.0	4.3	2.10	1.50	1.25	1.80	**Fail**
SW520GK	766	837	3.8	17.9	1.1	4.7	2.64	1.88	1.27	2.39	**Pass**
SW1020K	681	953	7.9	41.1	1.4	5.2	1.92	2.30	1.36	3.16	**Pass**
SW320KR6	205	270	1.7	8.6	1.3	5.0	2.47	1.65	1.25	2.06	**Fail**
SW320KR5	246	334	1.8	9.1	1.4	5.1	2.87	1.91	1.25	2.39	**Pass**

Note:

1) SSF obtained from FEMA P695 table for a given T and μ_T

2) ACMR = SSF (T, μ_T) × CMR

S_{MT} = 1.5g, 1.4g, and 0.83g for 3-, 5-, and 10-story archetypes, respectively.

3) Acceptance criteria: $ACMR_{10\%}$ for β_{TOT} of 0.6 = **2.16**

Pass if ACMR ≥ $ACMR_{10\%}$, otherwise Fail

5. Adjustments to Satisfy Collapse Performance of Balanced Archetypes

One possible adjustment to improve the balanced archetypes collapse performance is to design them with a lower value of the *R* factor and repeat the performance evaluation with the same collapse probability of 10% and total system collapse uncertainty (β_{TOT}) of 0.6. Here, this was done by designing another 3-story balanced archetype with *R* factor of 6. The archetype was denoted as SW320KR6 in Table 4 and its collapse fragility curve obtained from IDA is plotted in Fig. 3, superposed with the fragility curves for SW320 and SW320K. Interestingly, contrary to initial expectations, reducing the *R* factor from 7 to 6 did not result in a significant improvement in its performance. The calculated ACMR of 2.06 is approximately 5% below the acceptable $ACMR_{10\%}$ of 2.16. Although some could consider that difference acceptable, to be rigorous, another design iteration was performed using an *R* factor of 5; the resulting balanced archetype is denoted as SW320KR5. As hoped, SW320KR5 satisfied the performance criteria. Here, the calculated ACMR of 2.39 is 11% higher than the threshold $ACMR_{10\%}$.

Based on the above results, seismic performance factors for SPSW designed with $\kappa_{balanced}$ are recommended to be smaller compared to that for conventional SPSW (i.e., the 100% design case, κ = 1.0). Results above indicate that an *R* factor of 5 should be used for the design of balanced SPSWs. No system overstrength factor is available in balanced SPSWs (i.e., $\Omega_o = 1$). Like for conventional SPSWs, the C_d factor for balanced SPSWs should be taken as similar to the assigned *R* factor (i.e., $C_d = 5.0$).

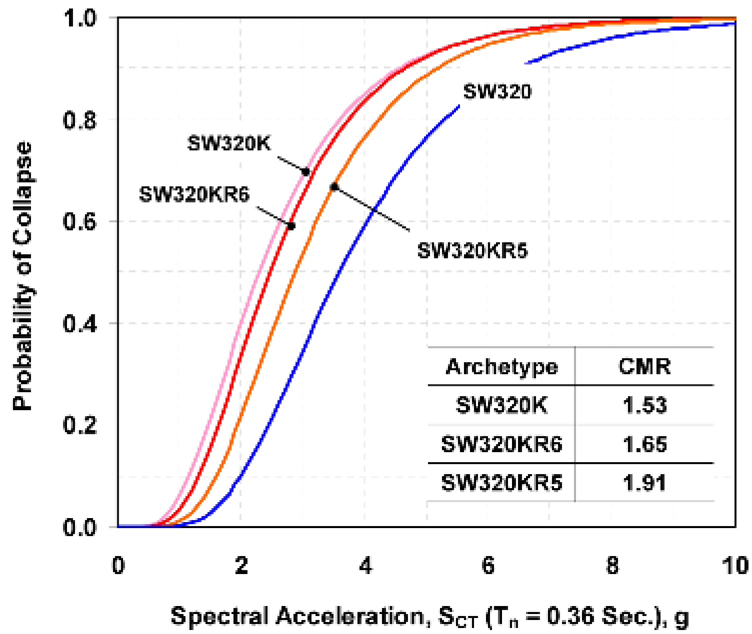

Fig. 3 – Fragility Curves for Archetypes with Different *R* Factors

6. Interstory Drift as Damage Measure (DM)

Considering the above results, it is also meaningful to interpret the IDA results in terms of drift demands. Specifically, fragility curves can be constructed for the probability of exceeding certain drift values in terms of spectral acceleration of the ground motions, for selected fixed values of interstory drifts up to the drift at the collapse. The resulting "drift-exceedance" fragility curves for SW320 and SW320K, using interstory drifts as DMs, are plotted in Figs 4a and 4b, respectively. As a reference, the results using the collapse point as the DM are superimposed in these curves. At the MCE level (i.e., S_{MT} = 1.5g), there is approximately a 50% probability that drifts will exceed 2% and 3.5% interstory drifts for SW320 and SW320K, respectively. More significantly at a 20% probability of exceedance, the respective archetypes will exceed 3% and 7% interstory drifts. The results indicate that SW320K has higher probability to suffer significant larger interstory drift, which can be associated with larger structural and non-structural damages. The same results were also obtained when comparing SW1020 and SW1020K in Figs. 4c and 4d.

It should be emphasized that even though the 10-story balanced archetype (i.e., SW1020K) had a calculated ACMR that met the acceptable ACMR limit, its probability to undergo significantly large interstory drift (i.e., ≥ 3%) can be as high as 50% under MCE ground motions (Fig. 4). While this SPSW designed with balanced case and *R* factor of 7 have sufficient margin to collapse, its ability to prevent damage to the structure and to drift-sensitive non-structural components is significantly less than for its counterpart archetype (i.e., SW1020). Hence, the need to design balanced archetypes with smaller *R* factor is deemed necessary.

In terms of the probability of exceeding the damage measures of 2, 3, and 4% interstory drift, results indicate that reducing the *R* factor from 7 to 6 resulted in an improvement of exceedance probability of no more than 10% for SW320KR6 compared to SW320K. More specifically, whereas half of the considered ground motions at the MCE level resulted in approximately 3.5% interstory drifts for SW320K, this slightly improved to 3.0% interstory drifts for SW320KR6. Moreover, half of the considered ground motions at the MCE level caused approximately 2.5% maximum interstory drifts for SW320KR5, which is tolerable and closer to what is expected for conventional SPSWs.

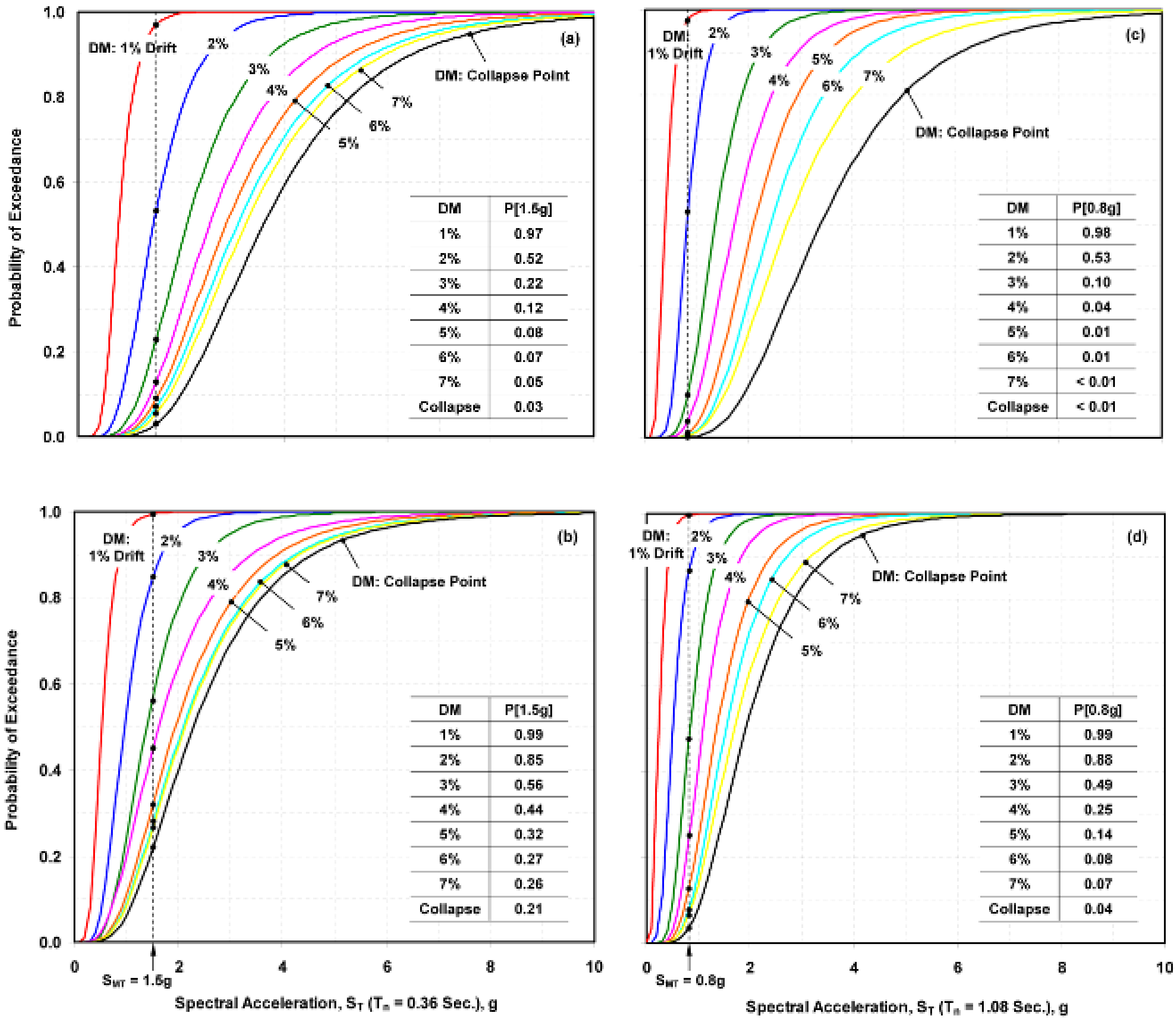

Fig. 4 – Exceedance Fragility Curves using Various Level of Inter-story Drift as Damage Measure: (a) SW320; (b) SW320K; (c) SW1020; (d) SW1020K

In terms of the total steel weight for archetypes designed with different *R* factors, the "reference" conventional SPSW (i.e., SW320, designed per [1] with an *R* factor of 7) requires a total of 10,459 pounds of steel. The case designed with $\kappa_{balanced}$ with *R* factor of 7, SW320K, requires a total of 5737 pounds of steel, which is approximately 55% less than what is required for the conventional design, but, as indicated above, SW320K did not meet the collapse performance criterion according to the FEMA P695 methodology and a lower *R* factor must be used. Designed with *R* factors of 6 and 5, SW320KR6 and SW320KR5 require 17 and 31% more steel than SW320K, but SW320KR5 still provides a 28% reduction in the total weight of steel from that is required for the conventional SPSW. However, that savings in steel comes at the cost of the SPSW designed for $\kappa_{balanced}$ developing larger interstory drifts compared to the conventional SPSWs (i.e., 2.5% versus 2.0% interstory drift) under MCE ground motions.

7. Impact of Archetype Configurations on Collapse Margin Ratio

In addition, results for the above twelve SPSW archetypes were compared to investigate how collapse performance would vary for various structural configurations. The resulting collapse fragility curves and the corresponding collapse margin ratios are presented in Fig. 5.

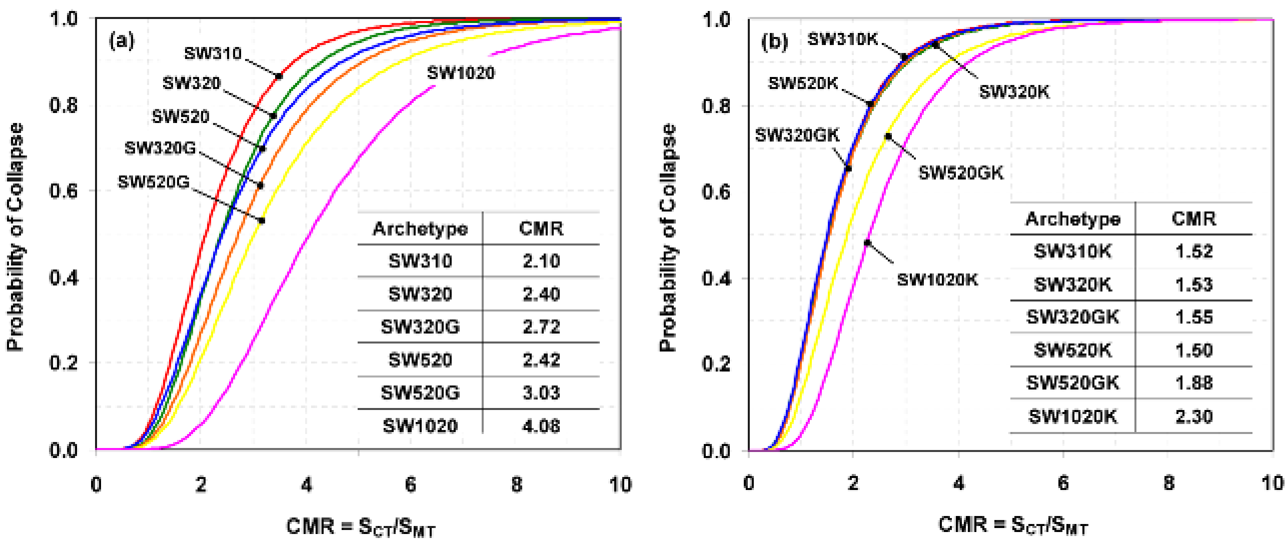

Fig. 5 – Collapse Fragility Curves for Archetypes with Various Configurations:
(a) 100% Design Case; (b) Balanced Design Case

7.1 Panel Aspect Ratio

As shown in Fig. 5a for the conventional design case ($\kappa = 1$), CMR for SW310 (i.e., 3-story archetype with panel aspect ratio of 1.0) is 2.10, which is 12.5% smaller than that of SW320 (i.e., 3-story archetype with panel aspect ratio of 2.0). This CMR for archetypes with smaller panel aspect ratio is reasonable that overstrength decreases as panel aspect ratio decreases. By contrast, the balanced archetypes (i.e., SW310K versus SW320K) have practically similar margins to collapse. As shown in Fig. 5b, their collapse fragility curves are on top of each other and their respective CMR values are 1.52 and 1.53. One might expect this result considering that both archetypes have the same minimum amount of overstrength.

7.2 Intensity Level of Seismic Weight

Initially, it was suspected that archetypes designed with high seismic weight would have lower (or, at worst, similar) margins to collapse compared to those with low seismic weight. This hypothesis was founded on the idea that the fundamental period of both archetypes would be comparable, because the ratio between their structural masses and stiffness would be similar (i.e., archetypes with low seismic weight would have smaller component sizes and therefore lower stiffness, while those with high seismic weight would have bigger component sizes and therefore higher stiffness). Interestingly, contrary to the initial expectation, the archetypes designed with higher seismic weight were found to actually have higher CMR values. This result can be observed in all cases considered (Fig. 5).

For this purpose, a series of monotonic pushover analyses were conducted to investigate the impact of P-Δ columns and deteriorated material models on archetypes designed with high and low seismic weights. The analyses were conducted on the 3- and 5-story archetypes as well as on the conventional and balanced design archetypes (i.e., total of 8 archetypes). Here, P-Δ has practically the same effects on both conventional and balanced archetypes irrespective of seismic weight intensity. When strength degradation was considered, high seismic weight had a more pronounced impact on the conventional archetypes compared to the balanced archetypes. Strength degradation occurred in SW520 at 1.9% top story drift while that in SW520G occurred at 2.4% top story drift. As for the balanced archetypes, SW320K and SW320GK experienced strength degradation at approximately 1.8 and 2.2% top story drift, respectively.

A subsequent investigation was directed to compare cross-section moment capacities of W-sections used for boundary elements of each archetype. In OpenSees model, the moment-rotation relationship at the cross section level was converted into a stress-strain relationship for fibers. In the absence of axial forces, given that the plastic hinge length is a function of the cross-section total depth, the furthest fiber from the neutral axis of any cross section reaches the same strain for a given cross-section rotation, irrespective of section depth. However, when axial force is present in a cross-section (which is typically the case for boundary elements), the degradation behavior of deep and shallow cross sections will vary because the axial load causes the neutral axis to move away from the center of gravity of the cross section. The larger the axial load the further the neutral axis shifts away from the center. For shallow cross-sections, the strain corresponding to the onset of degradation would be reached at a smaller rotation than that in deeper cross-sections, and strength degradation would take place faster.

As presented in Table 3, cross-section depths for the 3-story conventional archetypes designed with low and high seismic mass are significantly different. The latter case has relatively larger cross-sections. By contrast, that was not the case for the 3-story balanced archetypes. Both archetypes designed with low and high seismic mass have comparable sizes of HBEs and VBEs. Hence, the higher CMR values for archetypes designed with high seismic weight are an artifact of the selected boundary element sizes, and are not so much impacted by the P-Δ effect as initially predicted.

7.3 Number of Story

In general, CMR increases as the number of stories increase, irrespective of design approaches followed (i.e., conventional versus balanced design cases) and level of seismic weight intensity considered (i.e., low versus high seismic weight). The CMR increment however is not linearly corresponding to the increment of number of story.

The above result indicates that for the same intensity of ground motions, long-period archetypes have a lower probability to collapse compared to short-period archetypes. This finding is similarly observed when looking at examples in [5] for both reinforced concrete special moment frame and wood light-frame archetype systems, where short-period archetypes had lower value of CMR. In other words, to achieve the same level of collapse margin as long-period archetypes, short-period archetypes for these systems required additional strength or other form of modifications to improve their collapse performance [5].

8. Conclusions

Seismic performance of SPSWs having infill plates designed considering two different philosophies (i.e., conventional and balanced designs) was investigated using the FEMA P695 methodology. All conventional archetypes met the FEMA P695 performance criteria for the R factor of 7 used in their design. The Ω_o factor of 2 and C_d factor of 7 can be considered for conventional SPSW. The obtained seismic performance factors for conventional SPSW are somewhat similar to those specified in the ASCE 7-10 (i.e., R, Ω_o, and C_d factors are 7, 2, and 6, respectively). By contrast, the balanced archetypes designed with an R factor of 7 did not meet the FEMA P695 performance criteria. To rigorously meet the performance criteria, an R factor of 5 was required for the balanced SPSWs. No system overstrength factor was available for balanced SPSWs (i.e., $\Omega_o = 1$) and the C_d factor for balanced SPSWs should be taken similar to the assigned R factor.

Most importantly, the balanced archetypes were found to have a higher probability to suffer significantly larger (and unacceptable) interstory drift than the conventional archetypes. Savings in steel when designing balanced SPSWs with a lower R factor came at the cost of the SPSWs developing such larger interstory drifts compared to the conventional SPSWs under MCE ground motions. These findings suggest that the infill plates of SPSWs should be designed to resist the total specified story shears, rather than be designed by sharing those forces between the boundary frame and infill.

9. Acknowledgements

Incremental dynamic analyses were executed using the NEES-HUB supercomputer. This work was supported in part by the George E. Brown, Jr. Network for Earthquake Engineering Simulation (NEES) Program of the National Science Foundation under NSF NEESR Award Number CMMI-0830294. The financial support of the Fulbright Indonesia Presidential Scholarship and the Universitas Bandar Lampung, Indonesia to the first author is gratefully appreciated. However, any opinions, findings, conclusions, and recommendations presented in this paper are those of the writers and do not necessarily reflect the views of the sponsors.

10. References

[1] AISC (2010): Seismic Provisions for Structural Steel Buildings. ANSI/AISC 341-10, American Institute of Steel Construction, Inc., Chicago, Illinois.

[2] Canadian Standards Association (CSA) (2009): Design of Steel Structures. CAN/CSA S16-09, Willowdale, Ontario, Canada.

[3] Qu, B., and Bruneau, M. (2009): Design of Steel Plate Shear Walls Considering Boundary Frame Moment Resisting Action. *Journal of Structural Engineering*, ASCE, Vol. 135, No. 12, pp. 1511-1521.

[4] Bhowmick, A K., Driver, R. G., and Grondin, G. Y. (2011): Application of Indirect Capacity Design Principles for Seismic Design of Steel Plate Shear Walls. *Journal of Structural Engineering*, ASCE, Vol. 137, No. 4, pp. 521-530.

[5] FEMA. (2009): Quantification of Building Seismic Performance Factors. *FEMA Report No. P695*, Prepared by the Applied Technology Council for the Federal Emergency Management Agency, Washington, D.C.

[6] Vian, D., and Bruneau, M. (2005): Steel Plate Shear Walls for Seismic Design and Retrofit of Building Structures. *Tech. Rep. MCEER-05-0010*, Multidisciplinary Center for Earthquake Engineering Research, State University of New York at Buffalo, Buffalo, New York.

[7] Qu, B., and Bruneau. M. (2008): Seismic Behavior and Design of Boundary Frame Members of Steel Plate Shear Walls. *Technical Report MCEER-08-0012*, Multidisciplinary Center for Earthquake Engineering Research, Buffalo, New York.

[8] Choi, I-R., and Park, H-G. (2009): Steel Plate Shear Walls with Various Infill Plate Designs. *Journal of Structural Engineering*, ASCE, Vol. 135, No. 7, pp. 785-796.

[9] Driver, R. G., Kulak, G. L., Kennedy, D. J. L., and Elwi, A. E. (1997): Seismic Behavior of Steel Plate Shear Walls. *Structural Engineering Report 215*, Department of Civil Engineering, University of Alberta, Edmonton, Alberta, Canada.

[10] Purba, R., and Bruneau, M. (2014): Seismic Performance of Steel Plate Shear Walls Considering Various Design Approaches. *Tech. Rep. MCEER-14-0005*, Multidisciplinary Center for Earthquake Engineering Research, State University of New York at Buffalo, Buffalo, New York.

[11] Mazzoni, S., McKenna, F., Scott, M. H., and Fenves, G. L. (2009): Open System for Earthquake Engineering Simulation (OpenSees) User Command-Language Manual Version 2.0. Pacific Earthquake Engineering Research Center, University of California, Berkeley, Berkeley, CA.

[12] FEMA. (2000): State of the Art Report on Systems Performance of Steel Moment Frames Subject to Earthquake Ground Shaking. *FEMA Report No. 355C*, Prepared by the SAC Joint Venture Partnership for the Federal Emergency Management Agency, Washington, D.C.

[13] Purba, R., and Bruneau, M. (2012): Case Study on the Impact of Horizontal Boundary Elements Design on Seismic Behavior of Steel Plate Shear Walls. *Journal of Structural Engineering*, ASCE, Vol. 138, No. 5, pp. 645-657.

[14] PEER. (2005): PEER NGA Database. Pacific Earthquake Engineering Research Center (PEER), University of California, Berkeley, California. <http://peer.berkeley.edu/nga/>.

[15] Lubell, A. S., Prion, H. G. L., Ventura, C. E., and Rezai, M. (2000): Unstiffened Steel Plate Shear Wall Performance under Cyclic Loading. *Journal of Structural Engineering*, ASCE, Vol. 126, No. 4, pp. 453-460.

[16] Astaneh-Asl, A. and Zhao, Q. (2002): Cyclic Behavior of Steel Shear Wall Systems. *Proceedings*, Annual Stability Conference, Structural Stability Research Council, April, Seattle.

[17] Behbahanifard, M. R., Grondin, G. Y., and Elwi, A. E. (2003): Experimental and Numerical Investigation of Steel Plate Shear Wall. *Structural Engineering Report 254*, Department of Civil Engineering, University of Alberta, Edmonton, Alberta, Canada.

[18] Berman, J. W., and Bruneau, M. (2005): Experimental Investigation of Light-Gauge Steel Plate Shear Walls. *Journal of Structural Engineering*, ASCE, Vol. 131, No. 2, pp. 259 267.

[19] Park, H.G., Kwack, J.H., Jeon, S.W., Kim, W.K. and Choi, I.R. (2007): Framed Steel Plate Wall Behavior under Cyclic Lateral Loading. *Journal of Structural Engineering*, ASCE, Vol. 133, No. 3, pp. 378-388.

[20] Choi, I-R., and Park, H-G. (2008): Ductility and Energy Dissipation Capacity of Shear-Dominated Steel Plate Walls. *Journal of Structural Engineering*, ASCE, Vol. 134, No. 9, pp. 1495-1507.

[21] Li, C-H., Tsai, K-C, Lin, C-H, and Chen, P-C. (2010): Cyclic Tests of Four Two-Story Narrow Steel Plate Shear Walls. Part 2: Experimental Results and Design Implications. *Earthquake Engineering & Structural Dynamics*, Vol. 39, No. 7, pp. 801-826.